High-fidelity reprogramming into Leydig-like cells by CRISPR activation and paracrine factors

Zhaohui Li[a,1], Yuxiao Fan[a,1], Cankun Xie[a,1], Jierong Liu[a], Xiaoju Guan[b], Shijun Li[c], Yadong Huang [ID][a], Rong Zeng[d,*], Haolin Chen[b,*] and Zhijian Su[a,e,f,*]

[a]Guangdong Provincial Key Laboratory of Bioengineering Medicine, Department of Cell Biology, Jinan University, Guangzhou 510632, China
[b]Key Laboratory of Children Genitourinary Diseases of Wenzhou City, Department of Pediatric Urology, the Second Affiliated Hospital and Yuying Children's Hospital of Wenzhou Medical University, Wenzhou 325027, China
[c]Institute of Life Sciences, Wenzhou University, Wenzhou 325035, China
[d]Department of Material Science and Engineering, College of Chemistry and Materials Science, Jinan University, Guangzhou 510632, China
[e]National Engineering Research Center of Genetic Medicine, Jinan University, Guangzhou 510632, China
[f]Shaanxi Institute of Zoology, Xi'an, Shaanxi 710032, China.
*To whom correspondence should be addressed: Email: tjnuszj@jnu.edu.cn; chenhaolin@wmu.edu.cn; tzengronga@jnu.edu.cn
Edited By: Bruce Levine

Abstract

Androgen deficiency is a common medical conditions that affects males of all ages. Transplantation of testosterone-producing cells is a promising treatment for male hypogonadism. However, getting a cell source with the characteristics of Leydig cells (LCs) is still a challenge. Here, a high-efficiency reprogramming of skin-derived fibroblasts into functional Leydig-like cells (LLCs) based on epigenetic mechanism was described. By performing an integrated analysis of genome-wide DNA methylation and transcriptome profiling in LCs and fibroblasts, the potentially epigenetic-regulating steroidogenic genes and signaling pathways were identified. Then by using CRISPR/dCas9 activation system and signaling pathway regulators, the male- or female-derived fibroblasts were reprogrammed into LLCs with main LC-specific traits. Transcriptomic analysis further indicated that the correlation coefficients of global genes and transcription factors between LLCs and LCs were higher than 0.81 and 0.96, respectively. After transplantation in the testes of hypogonadal rodent models, LLCs increased serum testosterone concentration significantly. In type 2 diabetic rats model, LLCs which were transplanted in armpit, have the capability to restore the serum testosterone level and improve the hyperglycemia status. In conclusion, our approach enables skin-derived fibroblasts reprogramming into LLCs with high fidelity, providing a potential cell source for the therapeutics of male hypogonadism and metabolic-related comorbidities.

Keywords: male hypogonadism, Leydig-like cell, fibroblast, reprogramming, cellular therapy

---

Significance Statement:

Cell therapy is of fundamental importance for managing hypogonadism in future. Therefore, cell preparation is one of the most critical steps to ensure a successful and safe treatment. Using a combination of CRISPR activation and paracrine factors, the fibroblasts have been reprogramed into Leydig-like cells (LLCs). The cells are significantly close to real Leydig cells in phenotype and genotype. After transplantation to the sites inside or outside the testes, the cells could not only recover the serum testosterone concentrations, but also improve the hyperglycemia status in type 2 diabetic rat model. Our study found a more efficient way to make the competent LLCs and demonstrated in principal that reprogrammed LLCs have potentials to treat male hypogonadism and its-related metabolic comorbidities.

Introduction

Male hypogonadism, a common clinical syndrome caused by testosterone deficiency, can adversely affect multiple organ functions and quality of life (1). It is well established that low testosterone level can result in developmental abnormalities of the male reproductive tract, decreased fertility, sexual dysfunction, reduced muscle formation, osteoporosis, and cognitive dysfunction (2, 3). Clinically, male hypogonadism can be classified into primary, secondary, or mixed depending upon the etiology. Primary hypogonadism is the failure of the testes to produce sufficient testosterone despite of an elevated or unchanged luteinizing hormone (LH), whereas secondary hypogonadism involves pathology of the hypothalamus or pituitary that leads to decreased LH and subsequently testosterone (2–4).

In males, 90% to 95% testosterone is synthesized by Leydig cells (LCs), a process being regulated by the hypothalamus–pituitary–gonad (HPG) axis. Upon binding to its receptor (luteinizing hormone/choriogonadotropin receptor, LHCGR), blood

---

cholesterol is imported into LC and then transferred into mitochondrial inner membrane by scavenger receptor class B member 1 (SCARB1) and steroidogenic acute regulatory protein (StAR), respectively. After the catalysis of cytochrome p450 family 11 subfamily A member 1 (CYP11A1), cholesterol is converted into pregnenolone. This precursor of sex steroids is successively converted into testosterone by a series of enzymatic reactions mediated by 3β-hydroxysteroid dehydrogenase 1 (HSD3B1), cytochrome P450 17-alpha-hydroxylase/17,20-lyase (CYP17A1), and type 3 17β-hydroxysteroid dehydrogenase (HSD17B3) in the smooth endoplasmic reticulum (Figure S1A) (5, 6). It has been elaborated that the abnormalities in LC lineage development and/or steroidogenesis due to congenital or acquired causes can result in decreases of serum testosterone concentration (6–8).

The testosterone replacement is the most widely used approach for treating male hypogonadism so far. It has been approved for use in men with both primary or secondary hypogonadism to maintain secondary sex characteristics and relieve androgen deficiency-related symptoms (9). However, testosterone therapy is far from a perfect solution due to its potential adverse effects, such as reduced sperm production and fertility, promoting metastatic prostate cancer growth, and erythrocytosis (10). As a way to search an alternation, the Leydig-like cells (LLCs) were generated from different cell types and have them tested into laboratory animals (11–18). The precursor cells tested included embryonic stem cells (ESCs) (11), induced pluripotent stem cells (iPSCs) (12, 13), stem Leydig cells (SLCs) (14, 15), adult stem cells (ASCs) (16), and fibroblasts (17, 18). The LLCs generated from these sources were more or less effective in improving serum testosterone levels when transplanted into the hypogonadal animals.

However, making LLCs that are suitable for clinical usage is still challenging. The ideal LLCs should have key characteristics of real LCs, such as producing only desired steroids (T), responding to proper pituitary hormones (LH), with no tumor formation, and highly similar transcriptomic status with real LCs. However, for the most studies involving LLCs preparations described above (11–18), few addressed these issues. Here, we report a new way to make LLCs from mice tail tip fibroblasts (TTFs) based on targeted epigenetic reprogramming strategy that has better potential for *in-vivo* usage.

Results
Screening epigenetic regulatory factors during TTFs transdifferentiation to LLCs

To utilize the epigenetic-based approach to reprogram TTFs, we first profiled genome-wide DNA methylation level and transcriptome of TTFs and LCs using reduced representation bisulfite sequencing (RRBS) and RNA-Sequencing, respectively. For DNA methylation, differentially methylated regions (DMRs) were analyzed by examining the methdif value with $P < 0.001$ cutoff. A total of 20,074 DMRs were identified between TTF and LC libraries (Table S5). Of these DMRs, 719 regions were located within 442 gene promoters. For RNA-Sequencing, differential expression genes (DEGs) were selected by setting a threshold with a minimal 2-fold expression changes and false discovery rate (FDR) < 0.01. A total of 7,707 DEGs were found with 4,221 genes up-regulated and 3,486 genes down-regulated (Table S6). These results demonstrated that the global gene expression pattern of TTFs and LCs is distinctly different.

We next investigated the association between expression and DNA methylation status by integrative comparison of DMRs and

Table 1. Methylation and expression differences of steroidogenic genes between TTFs and LCs.

Gene name	MethDif[a] (P_value)	DMR (distance to TSS)	Fold change of mRNA[b] (P_value)
Nr5a1	−0.524 (1.61E-46)	Promoter (<1 kb)	8.533 (1.40E-76)
Lhcgr	−0.299 (7.97E-46)	Distal intergenic (−185 kb)	3.515 (6.21E-115)
Hsd17b3	−0.289 (4.45E-08)	Promoter (<1 kb)	7.814 (4.20E-09)
Scarb1	−0.258 (7.22E-31)	Distal intergenic (68 kb)	1.601 (7.15E-17)
Nr5a2	0.216 (2.65E-34)	Distal intergenic (−427 kb)	−3.639 (1.60E-10)
Nr1h3	0.267 (5.43E-16)	Promoter (1–2 kb)	−1.934 (4.60E-05)

[a]The value of methDif was presented by the different levels of DMR (TTFs versus LCs).
[b]The value of expression fold change was presented as log$_2$ format.

DEGs. A total of 3,228 DEGs containing 8,026 DMRs were identified. Among them, 2,159 genes with the inverse relationship of DNA methylation and mRNA expression were selected to perform Kyoto Encyclopedia of Genes and Genomes (KEGG) analysis. The significantly enriched processes included PI3K-Akt, Hippo, p53, Notch, cAMP, Hedgehog, and TGF-β signaling pathways (Figure 1A, Figure S1B). To further explore the relationships among these pathways, we selected 15 clusters with the best *P*-value to construct the network plot. Five signaling pathways, including PI3K-Akt, cAMP, Hippo, Hedgehog, and TGF-β were densely connected, suggesting their important roles in the conversion of TTFs to LLCs (Figure 1B and C). Based on this information, we used the agonists or antagonist for these five pathways during the reprogramming, including SAG, cAMP, LH, FGF-2, and ITS, and a TGF-β pathway inhibitor, LY2109761.

In addition, we further screened steroidogenic genes and the transcriptional factors in these DEG lists (Table 1). By evaluating the value of differentially methylation, the change of mRNA expression level and the function regulating LC differentiation (19), three steroidogenic genes, *Nr5a1*, *Hsd17b3*, and *Lhcgr*, were identified. Since none of them were expressed in fibroblasts in a meaningful level, a CRISPR/dCas9-VPR system with the capability of simultaneously changing the original expression status of multiple targeted genes was employed to activate their expressions during reprogramming.

gRNAs screening for activating endogenous steroidogenic genes in TTFs

NR5A1, LHCGR, and HSD17B3 are critical functional proteins for the development of LCs. LHCGR and HSD17B3 mediate the first and the last step in LH-stimulating testosterone production, respectively. NR5A1, an orphan nuclear receptor, plays essential roles in the development of the reproductive system and the differentiation of steroidogenic cells. To determine the activating effect of single gRNA on targeted genes, seven, four, and four gRNAs, which directly target the putative promoter regions of *Nr5a1*, *Lhcgr*, and *Hsd17b3*, respectively, were selected and delivered into TTFs (Figure 2A, Table S3). After cotransfection with CRISPR/dCas9-VPR, four gRNAs (the lh-gRNA1, lh-gRNA2, lh-gRNA3, and hsd-gRNA1) were able to sufficiently activate the expression of *Lhcgr* or *Hsd17b3*, respectively (Figure 2B). Interestingly,
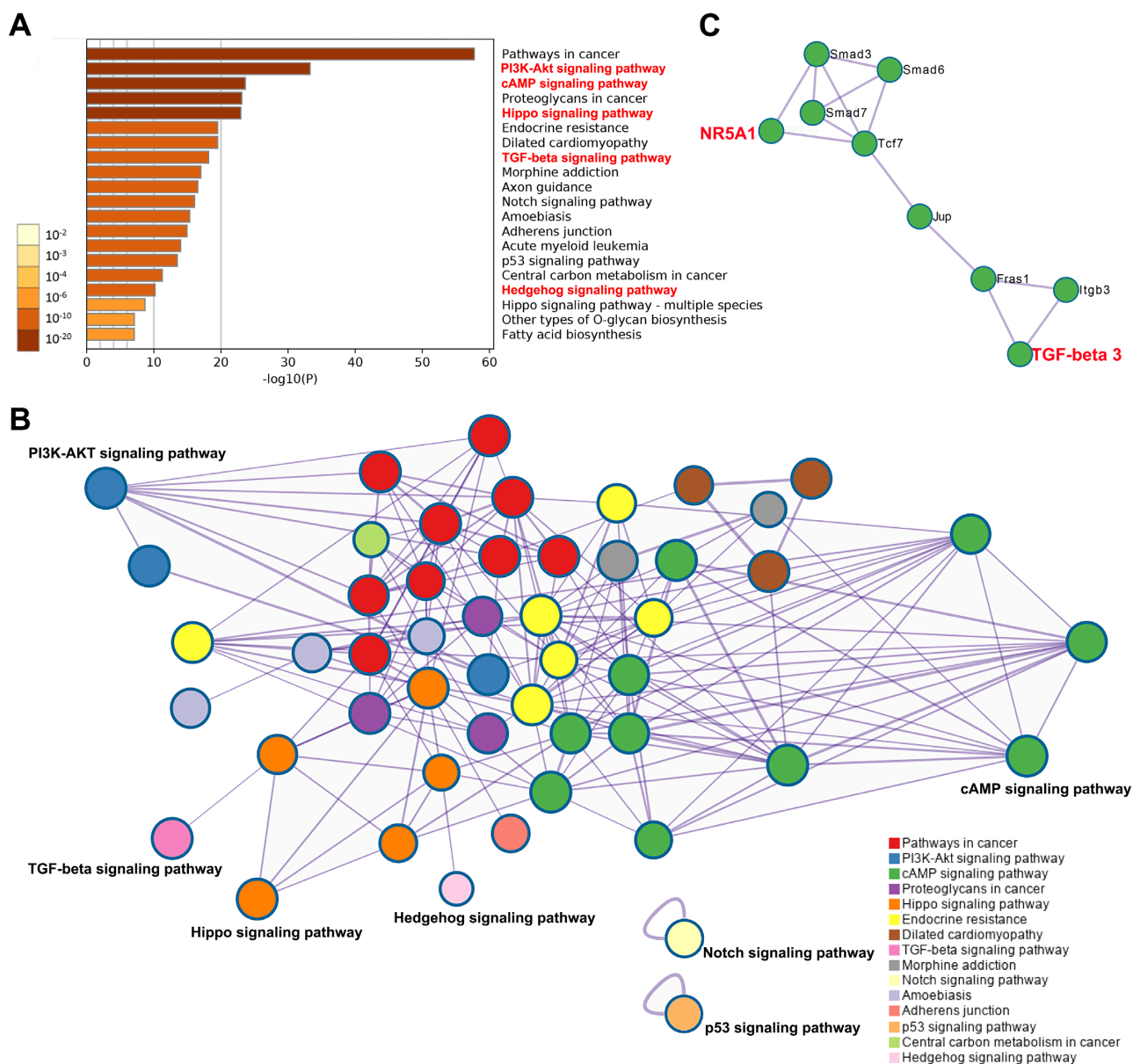
Figure 1. The functional enrichment analysis of genes with inverse relationships of expression and methylation between LCs and TTFs. (A) KEGG pathway enrichment analysis. The ordinate represents the most enriched KEGG pathways and the abscissa represents the P-value expressed as log10-transformed values. (B) The analysis of protein–protein interaction (PPI) network based on all enriched KEGG pathway terms. A subset of representative terms from the full cluster were selected and converted into a network layout. (C) The connection analysis of NR5A1 and TGF-β3. Each term is represented by a circle node, where the size is proportional to the number of input genes fall under that term, and the color represents the cluster identity. Nodes of the same color belong to the same cluster. Terms with a similarity score > 0.3 are linked by an edge whose thickness represents the similarity score.

the expression of *Hsd17b3* induced by hsd-gRNA1 was approximate 2.2-fold higher than that of LCs (Figure 2D). For *Nr5a1*, the activating ability of nr-gRNAs was low except nr-gRNA1. To optimize the activation, four best performing or seven gRNAs targeting *Nr5a1* promoter were concatenated into an all-in-one plasmid pool. The results indicated that the expression level of *Nr5a1* gradually increased depending on the numbers of gRNAs (Figure 2C).

To attain successful reprogramming, it is necessary to express the multiplex endogenous steroidogenic genes at high levels besides gRNA-targeted genes. Therefore, we arranged three plasmid combinations, that were cotransfected with CRISPR/dCas9-VPR into male-derived TTFs, to assess their activating efficiency (Figure S2A). The data shows that combination A and C not only

activated the expressions of *Lhcgr* and *Hsd17b3*, but also gradually increased the expression levels of *Cyp11a1*, *Hsd3b1*, *Cyp17a1*, and *Star* (Figure S2B).

Previous studies have shown that SAG, FGF-2, and cAMP played important role in LC lineage differentiation. Therefore, we further analyzed the promoting effects of LY2109761 and ITS, respectively. The qRT-PCR results demonstrated that 5 μM LY2109761 was able to significantly improve the expression of *Nr5a1* and steroidogenic genes with both plasmid combinations (Figure 3A). Similar results were also observed for ITS treatments (Figure 3B). Interestingly, after culture with ITS for 6 d, the originally elevated expressions of both *Cyp21a1*, an enzyme required for the synthesis of aldosterone in adrenal, and *Cyp19a1*, an enzyme being responsible for
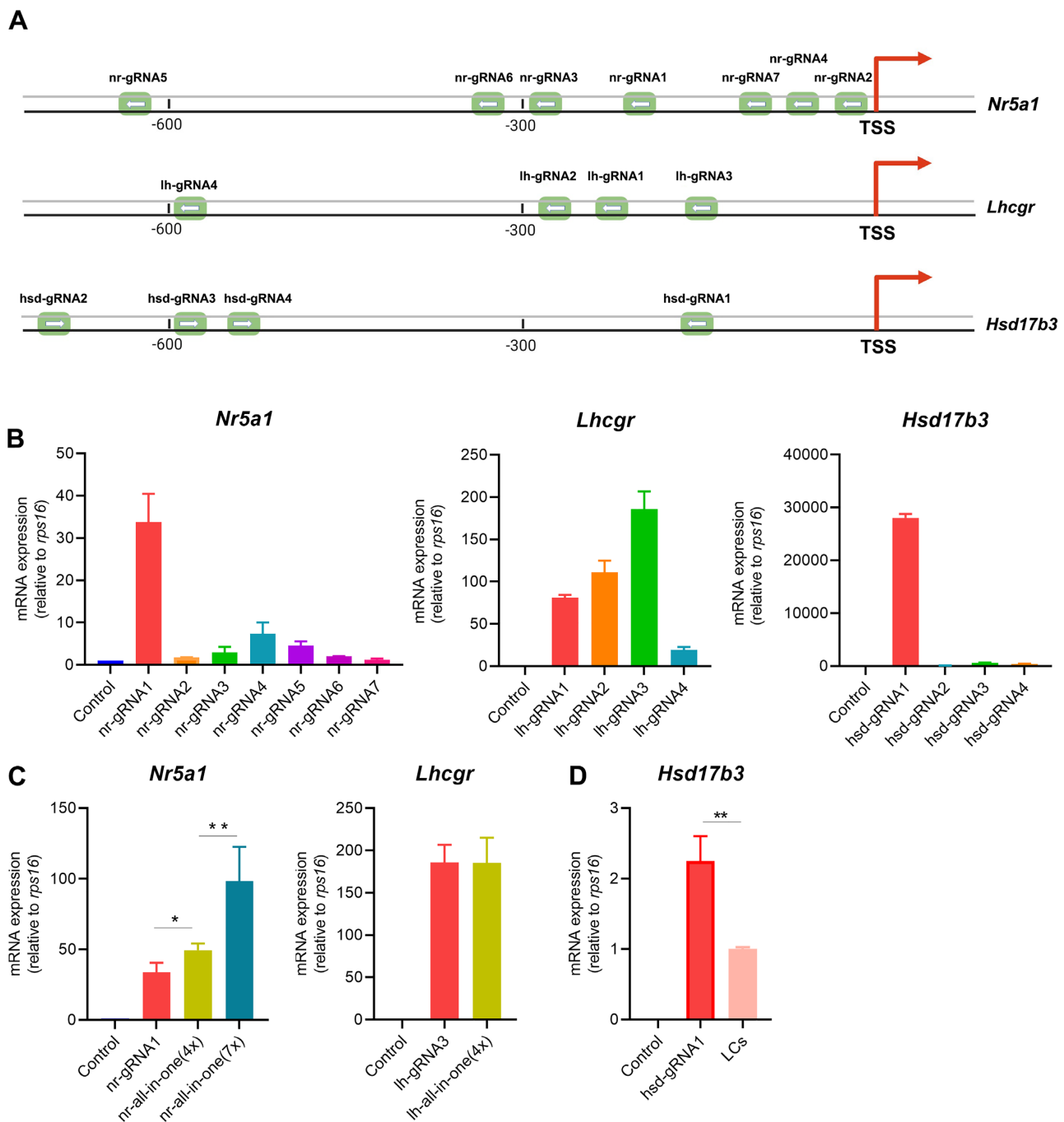
A

B

C

D

Figure 2. The optimization of dCas9-VPR activator and gRNAs targeting in TTFs for steroidogenic gene activation. (A) Promoter regions targeted by gRNAs for reprogramming genes (*Nr5a1*, *Lhcgr*, and *Hsd17b3*) in relation to their transcription start sites (TSS). (B) The activation of reprogramming genes detected by qRT-PCR, in TTFs 3 d after transiently expressed dCas9-VPR activator and single gRNA. (C) The activation of reprogramming genes detected by qRT-PCR, in TTFs 3 d after transiently expressed four or seven gRNAs and CRISPR/dCas9-VPR vector. (D) The expression of *Hsd17b3* between LCs and reprogramming cells. TTFs transfected with CRISPR/dCas9-VPR vector were used as Control. All quantitative data are from three independently treated samples and presented as mean ± SEM, $*P < 0.05$, $**P < 0.01$.

estrogen production in ovary, progressively decreased. In addition, the expression level of CRISPR/dCas9-VPR with/without signaling pathway regulators was similar, suggesting that the activation of these signaling pathway factors was not achieved by manipulating the expression of dCas9-VPR (Figure 3C). Considering the increasing expression of *Nr5a1* through gRNAs in a synergistic-effect and quantity-dependent manner, we selected the plasmid combination C for the remaining of this study.

Differentiation of TTFs into functional LLCs in vitro

The schematic approach for reprogramming TTFs is shown in Figure 4A. To examine whether the reprogram process mimics the real LC developmental process, different forms of androgens were monitored during the induction (Figure 4D). At early stage (day 6), LLCs produced high concentration of androsterone, with the average yield of 3.03 ± 0.29 ng/10^6cells/24 h. However, with the ex-
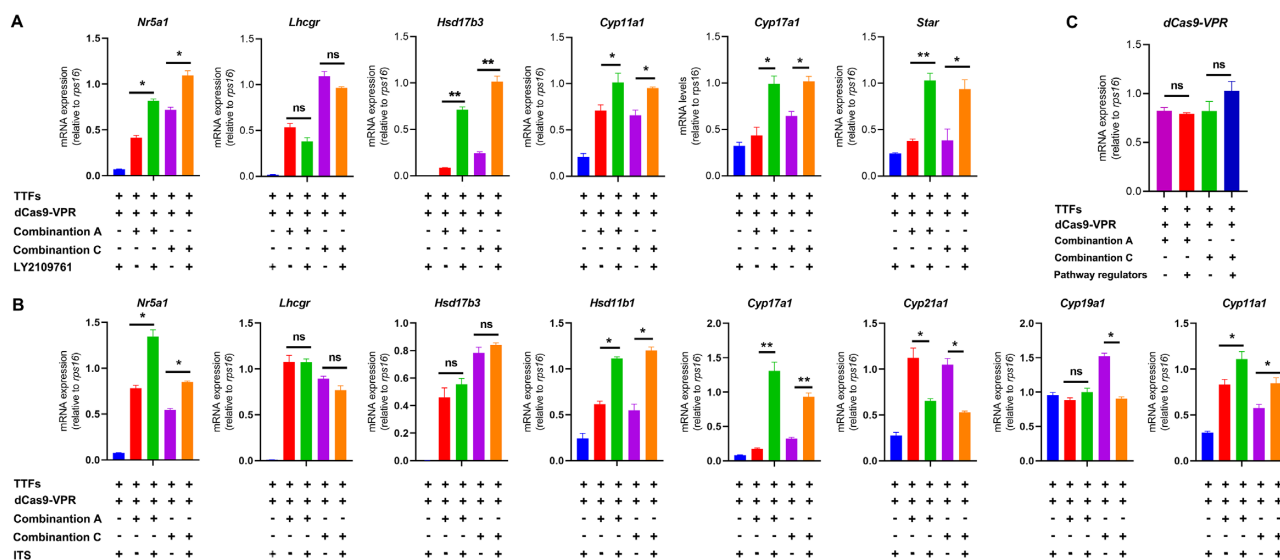
Figure 3. Expression of steroidogenic genes in TTFs treated by CRISPRa and signaling pathway regulators. (A) Expression of steroidogenic genes by CRISPRa and LY2109761. (B) Expression of steroidogenic genes by CRISPRa and ITS. (C) The analysis of dCas9-VPR expression. Combination A: plasmids for *Nr5a1* (4 gRNAs), *Lhcgr* (3 gRNAs), and *Hsd17b3* (1 gRNA); Combination C: plasmids for *Nr5a1* (7 gRNAs), *Lhcgr* (3 gRNAs), and *Hsd17b3* (1 gRNA). All quantitative data are from three independently treated samples and presented as mean ± SEM, $^{ns}P > 0.05$, $*P < 0.05$, and $**P < 0.01$.

tension of inducing process, androsterone decreased while testosterone increased dramatically. So by 12 d, the average concentration of testosterone reached 1.48 ± 0.15 ng/10^6cells/24 h, suggesting a similar maturation process as real LCs do (20).

Meanwhile, the expressions of androgen-synthesized genes, such as *Lhcgr*, *Star*, *Cpy11a1*, *Hsd3b1*, *Hsd17b3*, and *Cyp17a1*, all up-regulated (Figure 4B). The fibroblast markers, on the contrary, significantly decreased. The average expression levels of *Col5a2* and *Postn* reduced to 24% and 2.3%, respectively compared with the control (Figure 4C). Western blotting confirmed these expression results in proteins (Figure 4E). Furthermore, immunofluorescence staining shown that the expressed NR5A1, CYP11A1, and HSD17B3 were distributed on the appropriate locations in LLCs, meanwhile the ratio of positive cells was higher than 90% (Figure 4F). The signaling pathway regulators themselves could not activate TTFs to either produce testosterone or expressing endogenous steroidogenic genes, demonstrating the critical roles played by methylation/demethylation process during LLC reprogramming (Figure 4B and D).

To examine whether a gender may make a difference in the reprogramming, we also tried the female-derived TTFs as the starting cells. The qRT-PCR results indicated that the female cells are capable of expressing most steroidogenic genes except *Cyp17a1* (Figure 4G, Figure S3A). As a consequence, these reprogrammed cells lack of the ability to produce testosterone, suggesting an intrinsic gender difference in reprogramming (Figure 4H). In further examine whether rescue *Cyp17a1* expression can make the female cells to produce testosterone, we screened the gRNAs targeted the promoter of *Cyp17a1* and reconstructed the activating plasmid combination (Figure S3B to D). Eventually, the cells were capable of expressing all steroidogenic genes, including *Cyp17a1*, and producing testosterone (Figure 4I to J, Figure S3E to F). These results suggest that there is a gender difference in reprogramming androgen-producing cells. However, with a little extra effort, female-derived skin fibroblasts could also be successfully transdifferentiated into androgen-producing cells.

The LC characteristics of LLCs

The steroidogenesis of LC is strictly regulated by the HPG axis *in vivo*. Since both LH and hCG can bind to the LHCGR and subsequently trigger the testosterone synthesis, we examined whether our reprogrammed cells also responded to hCG stimulation. Culture of the LLCs with varying doses of hCG for 24 h resulted in different concentrations of testosterone in the media, indicating a dose-dependent response of the cells to hCG (Figure 5A).

Besides testosterone production, we also characterized the cells in more details. First, fully differentiated LCs lose their proliferating activity (7). With the cell reprogramming, the proliferative rate of LLCs significantly decreased compared to the TTFs. From day 10 to day 18, the proliferative curve of LLCs was gradually entering plateau phase, suggesting that the cell cycle had been arrested (Figure 5B). To confirm this conclusion, we analyzed the expression level of *Ccnd1*, one of LCs proliferative marker genes, in TTFs, LCs, and LLCs. The result indicated that the expression of *Ccnd1* in LLCs was 4.6-fold lower than that of TTFs after 18 d reprogramming (Figure 5C).

Second, insulin-like factor 3 (INSL3) is a peptide hormone constitutively produced uniquely by LCs in the testes of all mammals (21). The measurement of *Insl3* mRNA level indicated clearly that the reprogrammed cells were able to robustly produce INSL3, supporting the similarity of the LLCs and LCs (Figure 5D).

Third, LCs express HSD3B1 and contain lipid droplets in their cytoplasm. As judged by 3β-HSD histochemical staining and lipid staining, LLCs, not TTFs, presented these typical LC features (Figure 5E and F).

Fourth, in addition to testis, both the adrenal and the ovary also synthesize sex steroids, such as aldosterone and estrogen. Since all steroids share a basic structure and synthetic pathway, it is critical that the reprogrammed cells do not produce steroids undesired. *Cyp21a1* and *Cyp11b2*, which are important for aldosterone biosynthesis, and *Cyp19a1*, which converts testosterone into estrogen, were not increased significantly by reprogramming, with comparable low levels in both LLCs and TTFs (Figure 5G).
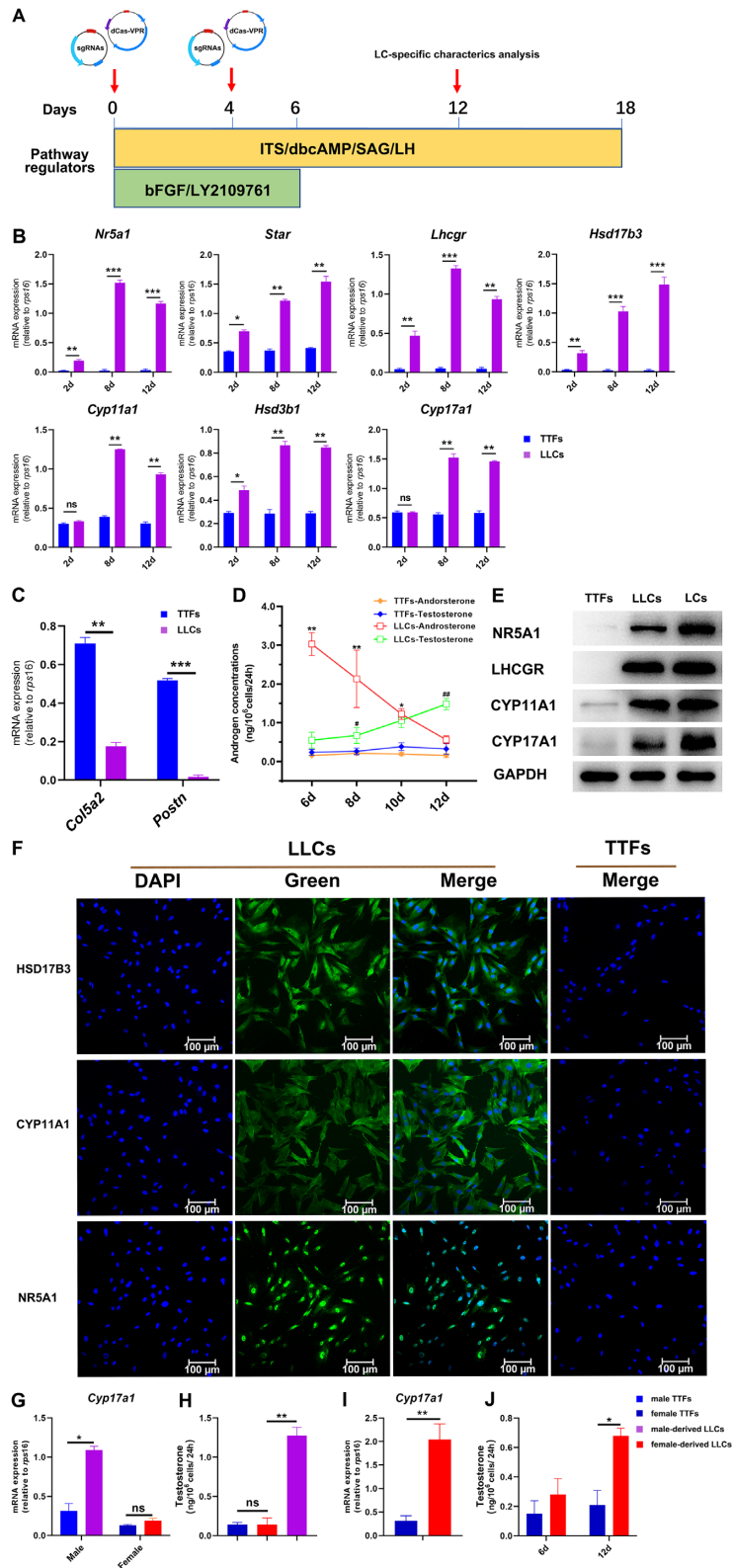
Figure 4. The expression of steroidogenic genes and androgen productions in LLCs during reprogramming. (A) Schematic representation of TTFs reprogramming with CRISPRa and signaling pathway regulators. (B) The expressions of steroidogenic genes during reprogramming. (C) The comparisons of fibroblast marker genes between TTFs and LLCs after 12 d reprogramming. (D) Shifts in androgen production during reprogramming ($*P < 0.05$ and $**P < 0.01$, LLCs versus TTFs for androsterone; $^{\#}P < 0.05$ and $^{\#\#}P < 0.01$, LLCs versus TTFs for testosterone). (E) Representative western blotting for the steroidogenic proteins after 12 d reprogramming. (F) Immunofluorescent staining of NR5A1, CYP11A1, and HSD17B3 in LLCs and TTFs after 12 d reprogramming. Nuclei were stained with DAPI (blue). Scale bars, 100 μm. (G, H) Gender effects on *Cyp17a1* expression and testosterone production after 12 d reprogramming. (I) The activation of *Cyp17a1* in female-derived TTFs using CRISPR/dCas9-VPR and gRNA plasmid containing cyp-gRNAs. (J) Testosterone productions of female-derived LLCs after reprogramming 6 and 12 d. All quantitative data were obtained from three independent experiments and presented as mean ± SEM, $^{ns}P > 0.05$, $*P < 0.05$, and $**P < 0.01$.
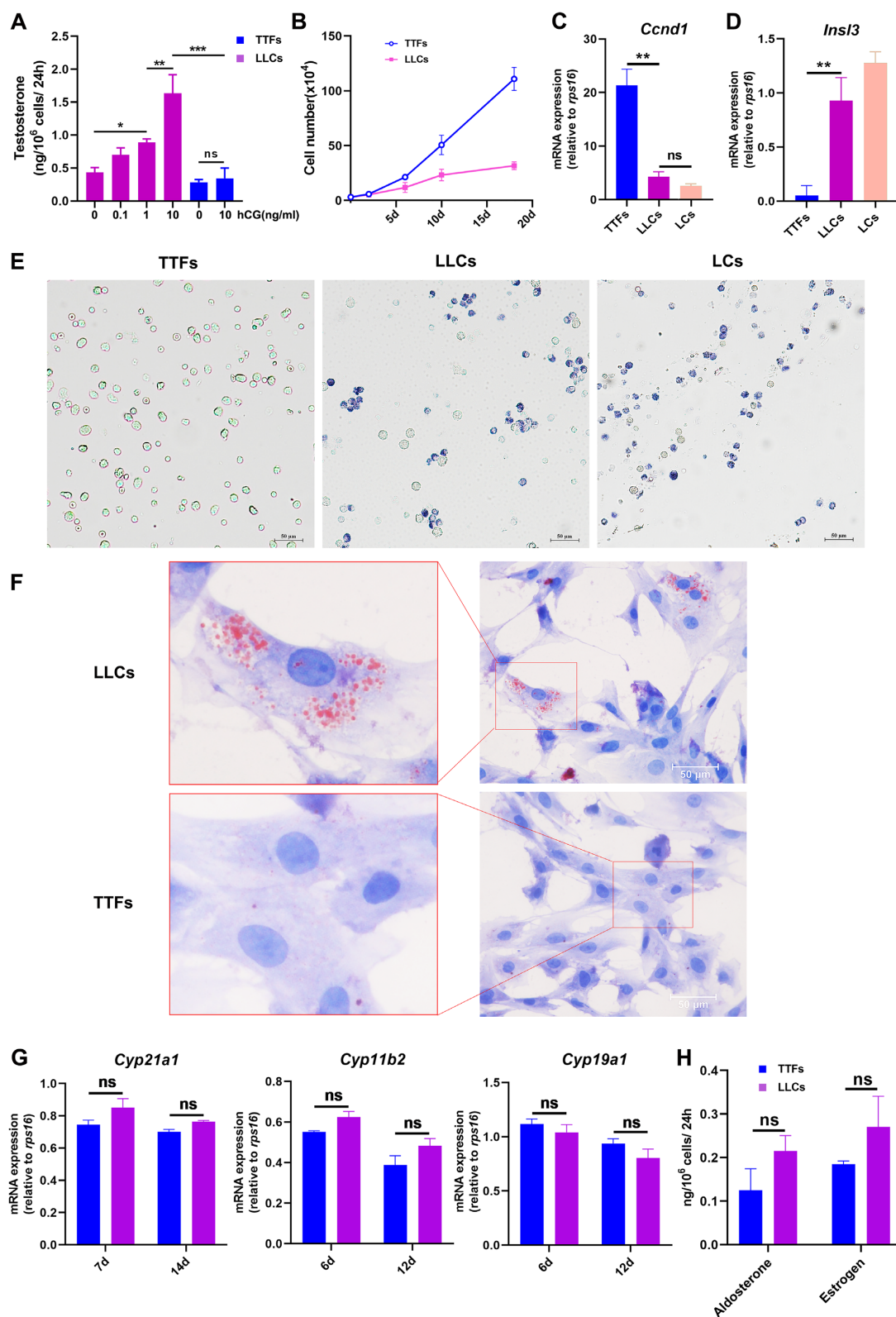
Figure 5. The assessment of LLCs for LC-specific characteristics. (A) The testosterone productions of LLCs in response to hCG doses. (B) The proliferation assays of TTFs and LLCs. (C, D) The mRNA expressions of *Ccnd1* and *Insl3* in TTFs, LLCs, and LCs. (E) HSD3B enzymatic staining (purple) for TTFs, LLCs, and LCs. (F) Oil red O staining (red) of lipids with hematoxylin counterstaining (blue) for TTFs and LLCs. (G) The mRNA expressions of *Cyp21a1*, *Cyp11b2*, and *Cyp19a1* for LLCs and TTFs at 6 and 12 d reprogramming. (H) The aldosterone and estrogen concentrations produced by LLCs after 12 d reprogramming. All quantitative data were obtained from three independent experiments and presented as mean ± SEM, $^{ns}P > 0.05$, $*P < 0.05$, $**P < 0.01$, and $***P < 0.001$. Scale bars, 50 μm.

Radioimmunoassay (RIA) results also confirmed that LLCs just produced trace amounts of aldosterone and estrogen (Figure 5H). In short, our procedure specifically reprogrammed TTFs into functional androgen-producing cells with LC-specific characteristics.

Transcriptomic analysis of LLCs

To further characterize LLCs, the transcriptomes of TTFs, LLCs, and LCs were investigated that detected a total of around 33,294 genes. The transcriptomic similarities and differences among the three groups were analyzed by Pearson's correlation coefficient and heatmap. The coefficients between LLCs and LCs are much higher (0.81 to 0.85) than these between LLCs and TTFs (0.32 to 0.58), confirming that LLCs is much closer to LCs than to TTFs (Figure 6A). Detailed analysis of 3,911 DEGs between TTFs and LLCs found 2,303 genes up-regulated in LLCs that contained all steroidogenic marker genes and 1,608 down-regulated genes that enriched fibroblasts marker genes (Table S7). A two-way hierarchical clustering analysis shown that the DEGs between LLCs and LCs were far more close to each other than to TTFs (Figure 6B). Clearly, LLCs displayed a distinct gene expression pattern compared to those of TTFs.

Changes in the TF expression pattern reflect cell fate decisions, therefore, we next investigated the tendency of TFs expression among LLCs, TTFs, and LCs. All the 1,237 TF genes were clustered and conducted the pairwise comparison (Table S8). The correlation coefficient between LLCs and LCs was higher than 0.96, suggesting the TFs expression pattern of LLCs is highly positive correlation with LCs (Figure 6C). The hierarchical clustering analysis further confirmed that the TF expression tendency of LLCs was close to that of LCs (Figure 6D). To evaluate the accuracy of sequencing data, several endogenous nuclear receptors involving in LC steroidogenesis were confirmed by qRT-PCR. Compared to TTFs, these TFs, such as *Nr4a3*, *Gata4*, and *Nr1h3*, were significantly up-regulated (Figure 6E). Importantly, the expression of dcas9-VPR was barely detected after induction for 12 d (Figure 6F). Collectively, these results confirmed that LLCs not only became steroidogenic, but also gained the main LC-specific phenotypes.

Transplantation of LLCs showed beneficial effects for treating hypogonadism

Reduction in LC numbers due to hypoplasia or apoptosis can result in lower testosterone output and hypogonadal phenotypes. To determine the therapeutic potential of LLCs, a primary hypogonadal model was constructed by injecting EDS to eliminate the existing LCs in mice testis (Figure 7A). Seven days after EDS-treated, the serum testosterone concentration of mice was decreased to a level barely detectable (0.078 ± 0.05 ng/ml). Subsequently, 2×10^6 LLCs were transplanted into the parenchyma of bilateral testes. Seven days after transplantation, serum testosterone levels of LLCs transplanted mice increased significantly compared to both model control and TTFs transplanted groups. By 14 d, the average serum testosterone concentration of LLCs animals was further recovered to approximated 75% of intact controls (Figure 7B).

In addition to mice, we also tested the therapeutic function of LLCs in EDS-treated rat model. Very similar to mice, transplantation of LLCs to EDS-treated rat testes also increased both serum and intratesticular testosterone levels (Figure 7C). To test whether the transplanted cells respond to pituitary regulation, we have injected the rats with hCG (10 IU) and monitored serum testosterone for 24 h (Figure 7D). Clearly, like the intact control rats, animals re-

ceived LLCs also responded to hCG stimulation by elevating serum testosterone levels in 2 and 6 h.

In human, in addition to reproduction, low testosterone in primary hypogonadism is also associated with other metabolic disorders, such as obesity and type 2 diabetes mellitus. We next assessed the potential therapeutic effects of LLCs on metabolic disorders of a type 2 diabetic rat model (Figure 7E). Four weeks after STZ treatment, the average fasting blood glucose (FBG) was about 17.38 ± 2.10 mmol/L in model rats, which was 3.1-fold higher than that of sham operation control (Figure S4A). The LLCs were encapsulated in a protective, semipermeable, cellulose-based bead and cultured for 24 h. The testosterone concentration in culture medium of encapsulated LLCs was similar to that of unpacked cells, indicating that the encapsulation did not affect the LH-mediated testosterone synthesis (Figure 7F). Transplantation of the LLCs-containing beads restored the circulating testosterone and TC to normal levels by 21 d after the transplantation (Figure 7G and H). Surprisingly, the administration of LLCs was also able to ameliorate hyperglycemia of diabetic animals sustainably with minimal changes in body weight (Figure 7I, Figure S4B). Although this effect was modest, the analysis of glucose tolerance and the hemoglobin A1C concentration confirmed that the blood glucose level and metabolic disorders of hyperglycemia were indeed improved by LLCs transplantation (Figure 7J and K, Figure S4C).

Discussion

Generating testosterone-producing LLCs by either differentiation of stem/progenitor cells or reprogramming of differentiated cells offers a promising therapeutic tool for treating human hypogonadism. Also, the studies provide unique opportunity to help us to understand the key regulatory mechanism involved in normal LC development. In this study, we demonstrate a rapid and robust approach to reprogram fibroblasts into LLCs with high fidelity by a combination of targeted activation of the selected endogenous steroidogenic genes and of key signaling pathways by exogenous molecules.

The methods of reprogramming or transdifferentiation can be classified into precise gene regulation and general induction. The former involves the precise activation of a few key TFs that will eventually change the fate of the cells. The latter strategy, on the contrary, usually needs an array of hormones, growth factors, and/or small signal modifying compounds. For reprogramming efficiency and steroidogenic capacity of LLCs, the method of gene regulation, especially based on activation of TFs, is markedly better than other strategies (22). Importantly, the ratio of LCs characteristics possessed by LLCs directly determines whether they are suitable for *in-vivo* transplantation. To implement the high-fidelity reprogramming, it is critical to alter the expression pattern of global genes, especially TFs, in starting cells to mimic that of LCs. We analyzed the associations between gene expressions and DNA methylations and focused on five signaling pathways, including PI3K-Akt, cAMP, Hippo, Hedgehog, and TGF-β. It has been reported that the small chemicals, such as SAG, cAMP, forskolin, and lithium chloride, and the biomolecules, such as LH, insulin, IGF-1, and growth factors, play important roles in the differentiation or transdifferentiation of various cells into LLCs (13, 15, 18, 23–27). The selection of LY2109761, an inhibitor of TGF-β signaling pathway, was mainly based on two bioinformatic evidences: (1) The KEGG results indicated that one of the targets enriched for DEGs between TTFs and LCs was TGF-β receptor (TGFβR) type II. (2) GO annotations shown the significant
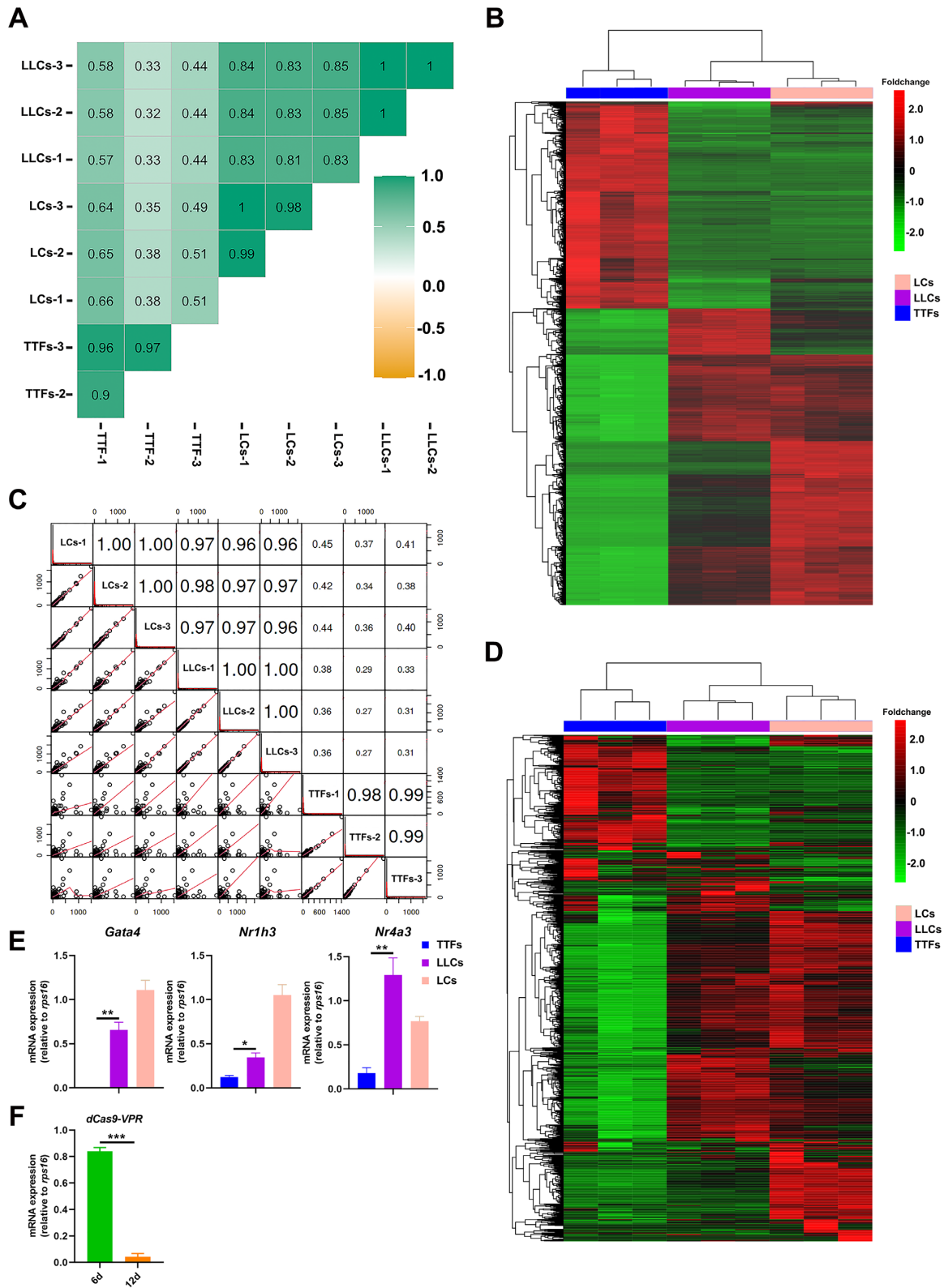
Figure 6. Transcriptional analysis of LLCs at day 12 of reprogramming. (A) The Pearson correlations among TTFs, LLCs, and LCs based on 33,294 global genes. (B) Heatmap comparsions of 3,911 DEGs for TTFs, LLCs, and LCs. The scale bar is in $\log_{10}$ format. (C) Scatter-plots and Pearson correlations of 1,237 TFs for TTFs, LLCs, and LCs. The numbers in the up-right diagonal of the plot matrix are the Pearson correlation coefficients. (D) Heatmap of all TFs for TTFs, LLCs, and LCs. The scale bar is in $\log_{10}$ format. (E) Expression of endogenous transcription factor (TF) genes (*Gata4*, *Nr1h3*, and *Nr4a3*) after 12 d reprogramming. (F) Expression of dCas9-VPR mRNA at 6 and 12 d reprogramming. All quantitative data, except as noted, were obtained from three independent experiments and presented as mean ± SEM, $*P < 0.05$, $**P < 0.01$, and $***P < 0.001$.
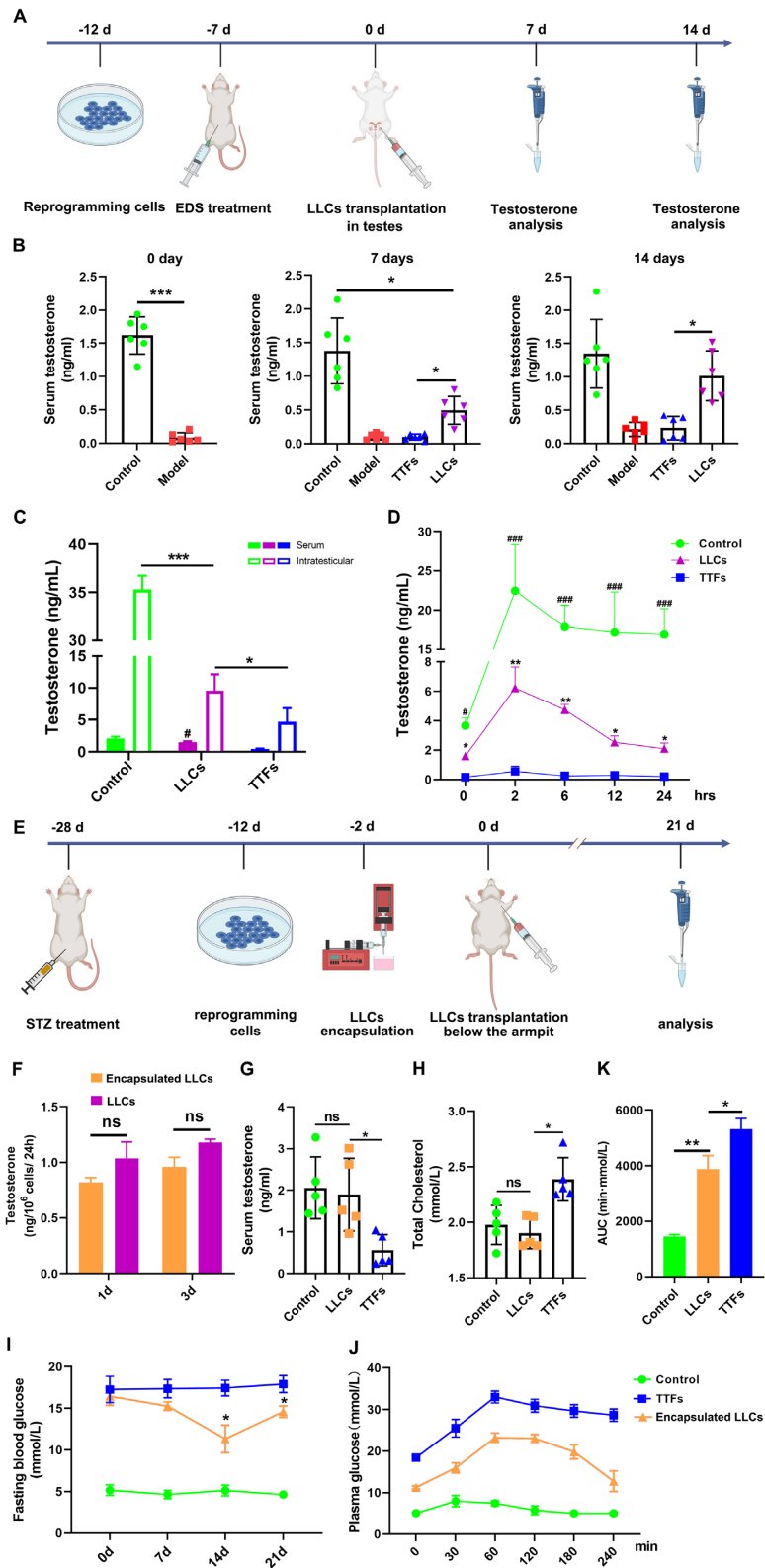
Figure 7. The functional assay of LLCs transplanted in hypogonadal rodent models. (A) Experimental procedure for LLCs transplantation in the testis of LC-depleted mice. (B) Time course of testosterone recovery after LLCs transplantation for the EDS-treated mice. ($n = 6$; one-way ANOVA, $*P < 0.05$, $**P < 0.01$, $***P < 0.001$). (C) Serum and intratesticular testosterone concentrations maintained by LLCs after transplantation for 21 d ($^{#}P < 0.05$, versus TTFs). (D) Serum testosterone levels in response to hCG administration for three groups of animals *in vivo* ($*P < 0.05$, $**P < 0.01$, LLCs versus TTFs; $^{#}P < 0.05$, $^{###}P < 0.001$, LCs versus LLCs). (E) Experimental procedure for subcutaneous LLCs transplantation to armpit of type 2 diabetic rats. (F) Testosterone productions by LLCs and encapsulated LLCs for 1 and 3 d in culture. (G) Testosterone concentrations of type 2 diabetic rats received LLCs or TTFs for 21 d. (H) Serum total cholesterol (TC) of type 2 diabetic rats received LLCs and TTFs for 21 d. (I) Blood glucose concentrations at 0, 7, 14, and 21 d after LLCs transplantation ($n = 5$; one-way ANOVA, $*P < 0.05$, versus TTFs). (J) Blood glucose levels of an oral glucose tolerance test (OGTT) performed on rats 21 d after transplantation ($n = 5$). (K) Blood glucose AUC statistics. All quantitative data, except as noted, were obtained from three independent experiments or five individual animals and presented as mean ± SEM, $^{ns}P > 0.05$, $*P < 0.05$, $**P < 0.01$, and $***P < 0.001$.

enrichments of DEGs in collagen-containing extracellular matrix and epithelial cell proliferation that often related to TGF-β signaling. Our results have proven that application of LY2109761 not only increased the expression of steroidogenic genes, but also suppressed the proliferation of induced cells. However, the elongated treatment of LY2109761 resulted in cell apoptosis. Adding FGF-2 simultaneously was effectively prevented such side effect, which was probably due to the fact that FGF-2 is a potent mitogen with a capacity of antiapoptosis (28).

NR5A1 has been shown repeatedly to be critically required for the successful differentiation of various stem cells and fibroblasts into LLCs (22, 29). Unlike *Lhcgr* and *Hsd17b3*, the current study found that it was difficult to sustain a high-level *Nr5a1* expression by CRISPRa system with a single gRNA. The reason may relate to the selection of gRNAs. To avoid the off-target effect, we preferentially selected the higher specificity score of gRNAs binding to the promoter region. Unfortunately, most of them were with lower activating efficiency. Therefore, the decision to deliver seven gRNAs for *Nr5a1* activation was made according to the synergistic effects of multiple gRNAs (30, 31). With such a strategy, we were able to get a robust expression of *Nr5a1*.

Both male and female sex steroid hormones share very similar structure and the synthetic pathways, therefore, we want to know whether gender makes a difference in the reprogram of TTFs. The female-derived cells were able to express all steroidogenic genes up to testosterone except *Cyp17a1*. With an extra step to stimulate *Cyp17a1* expression, female TTFs were successfully reprogrammed into testosterone-producing LLCs. But, overall, the efficiency of transformation and testosterone-producing ability were significantly lower than those of male-derived cells. The differences between the two genders and the mechanisms involved deserve further investigation. It is possible that the sex chromosome plays an important role in the transdifferentiation process, and the female-derived LLCs may have higher propensity to form ovarian steroidogenic cells (32–34).

Multiple generations of LCs have been identified in mammalian testes. For rodents, the postnatal development of the adult LC population undergoes four phases: stem Leydig cells (SLCs), progenitor Leydig cells (PLCs), immature Leydig cells (ILCs), and adult Leydig cells (ALCs). SLCs do not synthesize any androgens, while PLCs, ILCs, and ALCs produce androsterone, 5α-androstane-3α,17β-diol, and testosterone as final product, respectively (20, 35). During induction *in vitro*, the major androgen produced by LLCs transformed quickly from androsterone to testosterone, suggesting that the reprogramming of LLCs implemented a similar developmental process of LC lineage *in vivo*.

In this study, transplantation of LLCs inside or outside the testis were able to survive and increase the serum testosterone concentration, indicating that the niche of testicular interstitium is not a must for the survival and functions of transplanted LLCs. If not considering spermatogenesis, it could be more feasible, easier to accept, and less damaging to the reproductive organ with transplantation of LLCs outside the testis. As for the lower intratesticular testosterone concentrations obtained by LLCs-treated animals than these of intact control group, the reason may relate to the fewer LLCs transplanted compared to the full LC population generated naturally (about 70 million LCs in both rat testes) (36).

Androgen plays an important role not only in reproduction, but also in general metabolism of the body. Androgen deficiency results in reduced fertility, sexual dysfunction, decreased muscle formation and bone mineralization, disturbances of fat metabolism, and cognitive dysfunction (37). Moreover, low testosterone level and the major metabolic diseases such as type 2 diabetes mellitus, metabolic syndrome, cardiovascular disease, and osteoporosis appear closely connected, forming a vicious cycle that leads to further hypogonadism (38). Clinically, testosterone deficiency is associated with impaired fasting glucose and insulin resistance in diabetic males, while supplementation of testosterone can promote insulin sensitivity and maintain glucose homeostasis. Our results indicated that the blood glucose concentration of STZ-treated rats was improved sustainably in accompanied with the restoration of testosterone level by LLCs. This insulinotropic effect of testosterone may be related to the stimulation of islet insulin synthesis or the activation of the androgen receptors to enhance glucose-stimulated insulin secretion (39–42) among others.

In summary, we established an epigenetic strategy to reprogram rat skin-derived fibroblasts into LLCs with high fidelity. The cells gained much better traits of real LCs. The transplantation of LLCs inside or outside the testis can significantly restore serum testosterone in hypogonadal models. Moreover, the LLCs have the therapeutic potential for diabetes remission. By optimizing gRNA combinations and signaling pathway modulators, this approach may also be feasible in reprogramming human fibroblasts into functional LLCs. Our study lays a foundation for the development of human LLCs for the future clinical application in treating male hypogonadism and metabolic disorders.

Materials and methods
Chemicals and reagents
Information about chemicals, cell culture media, antibodies, primers of quantitative polymerase chain reaction, and primers for constructing the expression cassette of guide RNAs (gRNAs) are summarized in Table S1 to S4.

Isolation and culture of TTFs and LCs
The tail tip dermal fibroblasts (TTFs) were isolated from the adult male SD rat (postnatal 90 d). Briefly, three tails were sterilized with 70% ethanol and rinsed three times with PBS. Then the outside skin was removed from the tails and minced into 0.2 to 0.5 cm pieces with scissors. These fragments were placed into T75 cell culture flasks, added 10 mL expanding media (DMEM containing 10% FBS and 1% antibiotic solution) and cultured at 37°C for 4 d. The tail tissues were then removed without disturbing the adherent fibroblasts. The cells were splitting 1:3 for passaging with 0.05% trypsin for 1 to 2 min when they reached 90% confluence.

For the isolation of primary LCs, testes of 40 postnatal 21 d rats were enzymatically dispersed with 0.25 mg/mL collagenase D in Medium 199 for 10 min at 34°C. The dispersed cells were filtered through two layers of 100-μm pore size nylon mesh, centrifuged at 250 × *g* for 10 min, and resuspended in 55% isotonic Percoll to separate cells by buoyant density. After centrifugation at 23,500 × *g* for 45 min at 4°C, the fraction of LCs with densities between 1.068 and 1.070 g/mL was collected. The purity of isolated LCs was more than 93% according to the 3β-hydroxysteroid dehydrogenase (3βHSD) activity staining.

The analyses of whole genome methylation and transcriptome of the TTFs on passage 2 to 3 and the freshly isolated LCs, were performed by Biomarker Technologies Corporation, Beijing, China (http://www.biomarker.com.cn/).

DNA methylation analysis and DMGs detection
DNA was extracted from TTFs and LCs using cetyltrimethyl ammonium bromide (CTAB) following standard procedure. DNA

methylation library was constructed and analyzed by reduced representation bisulfite sequencing (RRBS) on Illumina HiSeq X Ten (Illumina Inc., San Diego, CA, USA) platform. Raw data were preprocessed using the pipeline. Sequencing data were first trimmed and aligned to Genome Reference using Trim Galore and Bowtie2, respectively (43, 44). The coverage outputs from Bismark were imported to R package BiSeq to smooth the methylation level. DMRs were identified using software (45). The different level of DMRs between the TTFs and the LCs was evaluated by methdif value (TTFs versus LCs). The DMRs with methdif value less than −0.2 or higher than 0.2 were classified as hypomethylation and hypermethylation regions, respectively. Then, DMGs were defined as genes whose promoter or gene body regions overlapped with single or multiple DMRs (46).

DEGs detection and their integrative analysis with DMGs

Samples for RRBS were also done for transcriptomic analysis. Total RNA was extracted from each sample by TRlzol reagent according to the instruction manual and the mRNA was isolated subsequently. The cDNA libraries were constructed, and sequenced by an Illumina HiSeq platform. DESeq and the FDR-adjusted P-value were employed and used to evaluate DEGs based on the ratio of the fragments per kilobase of exon per million fragments mapped (FPKM) values. The DEGs (TTFs versus LCs) were identified and then divided into up- and down-expression groups with fold change value ≥ 2 or ≤ 0.5, and P-value < 0.01.

The enrichment analysis of KEGG pathway was performed using the genes with the inverse relationship of expression and methylation (TTFs versus LCs). For PPI enrichment, the analysis was carried out with the databases STRING and BioGrid and shown through the resultant network containing the subset of proteins that form physical and functional interactions. These enrichment analyses were performed by METASCAPE (version 3.5, https://metascape.org/) (47) and DAVID software (Database for Annotation, Visualization and Integrated Discovery, version 6.8, http://david.abcc.ncifcrf.gov/).

Construction of the gRNAs expression vectors

The single or all-in-one gRNAs expression vectors were constructed according to the instructions of multiplex CRISPR/Cas9 assembly systems kit with some modification (48). Briefly, the original vectors in kit, pX330A-dCas9-1 × 7 and pX330A-dCas9-1 × 4, were digested using EcoR V and P*ml* l endonucleases to destroy the dCas9 gene. These treated vectors were named pX330A-1 × 7 and pX330A-1 × 4, respectively. The gRNAs targeted the promoters of *Nr5a1*, *Lhcgr*, and *Hsd17b3* were obtained from the on-line protocol (http://crispr-era.stanford.edu/index.jsp). The detailed procedure for constructing gRNA vectors can be found in Supplementary Material.

The activation of targeted genes mediated by CRISPRa or signaling pathway regulators

The TTFs were prepared from 10 male or female rats (postnatal day 7) and used within three passages. To evaluate the activating effect of targeted genes, TTFs were inoculated to 6-well plates (3×10^5 cells/well) in DMEM/F12 with 10% FBS and cultured for 12 h. Total of 2.5 μg DNA of PB-TRE-dCas9-VPR and recombinant gRNA vectors was transfected into the TTFs according to the instruction of Lipofectamine 3000 reagent. After 6 h incubation, the medium was replaced with fresh DMEM/F12 with 10% FBS, and changed every 2 d.

To evaluate the activating function of signaling pathway regulators, the TTFs were cultured with reprogram inducing medium (DMEM-F12 containing 10% FBS, 0.5 μM SAG, 10 ng/mL LH, 1 mM dbcAMP, 10 ng/mL FGF-2, and 1 × ITS) for 6 d. The medium was replaced every other day. For the evaluation of TGF-β signaling pathway, TGF-β inhibitor LY2109761 (5 μM or 10 μM) was added into the medium. Then, the TTFs were transfected with CRISPR-activating combinations and cultured with inducing medium containing LY2109761 for 6 d. All experiments described above were repeated three times and the expression of steroidogenic genes was analyzed by qRT-PCR.

The generation of LLCs

The schematic illustration of differentiating stages from TTFs into LLCs is shown in Figure 4A. On stage 1, TTFs were cultured in 6-well plates (3×10^5 cells/well) with DMEM-F12 containing 10% FBS and incubated for 12 h at 37°C under 5% CO_2. Then the cells were transfected with the reprogramming vector combinational solution (1.8 μg PB-TRE-dCas9-VPR and 0.7 μg all-in-one gRNA expression vectors) by Lipofectamine 3000 for 6 h. Discarded the medium, the cells were cultured with reprogram inducing media 1 (namely RIM 1, DMEM/F12, 10% FBS, 0.5 μM SAG, 10 ng/mL LH, 1 mM dbcAMP, 10 ng/mL FGF-2, 5 μM LY2109761, and 1 × ITS) for 3 d. On day 4, when the cells reached ∼90% confluence, they were digested and reseeding into 6-well plates (3×10^5 cells/well), the second transfection was conducted. Similar to the protocol of first transfection, the cells were continuously inoculated with re-programming vectors and cultured with RIM1 for 2 d. On stage 2, the reprogram inducing media 2 (namely RIM 2, DMEM/F12, 10% FBS, 0.5 μM SAG, 10 ng/mL LH, 1 mM dbcAMP, and 1 × ITS) were used to promote the cells differentiation into LLCs. This cultural stage lasted 6 to 12 d and the medium was changed every 2 d. After reprogramming, the functional analysis and RNA-Sequencing were performed for LLCs and TTFs.

Androgen assays by UHPLC-MS/MS

The culture media of LLCs were collected at day 6, 8, 10, and 12 of reprogramming process. Androsterone and testosterone were assayed simultaneously by ultra-high-performance liquid chromatography coupled with triple quadrupole mass spectrometry method (UHPLC-MS/MS) (49). In brief, 180 μL media of each sample were mixed with 90 μl methanol and 90 μl steroids solution containing ethinylestradiol (450 pg/mL) and norethisterone (1 ng/mL). After adding 1.2 mL methyl-*tert*-butyl ether and vortex for 2 min, the upper organic phase was separated and evaporated using nitrogen. The dried residue was dissolved in methanol and performed the analysis. The assay sensitivities of androsterone and testosterone were 0.002 μg/L and 0.005 μg/L, respectively. The data were collected in centroid mode and processed using Masslynx 4.1 software and Quanlynx program (Waters Co.). The results from four separated experiments were averaged for the statistical analysis.

The RIA of testosterone, estradiol, and aldosterone

The RIA of the steroid concentration was performed as described previously. Briefly, the standards, controls, and samples (50 μL, in duplicate) were dispensed into numbered tubes. Subsequently, 100 μL of the I^{125}-labeled tracer and 100 μL of the primary antibody were added to the appropriate tubes. The tubes were shaken for 10 s and incubated in a water bath for 1 to 3 h at 37°C. Then, 500 μL of the secondary antibody was added to all of the tubes (except

the total count tubes), and the mixture was incubated for 15 min at room temperature. The tubes were then centrifuged at $1800 \times g$ and 4°C for 15 min. The supernatants were decanted, and the radioactivity in the precipitate was counted for 1 min. The sensitivity of the assay systems was less than 0.05 μg/L. The intra-assay and inter-assay variations were less than 10% and 15%, respectively.

Transplantation of LLCs in vivo

The "LC knock-out" rodent models were used to test the effect of LLCs on the treatment of primary hypogonadism (17). To eliminate existing LC population, a single intraperitoneal injection of EDS (100 mg/kg) were administered to adult C57BL/6 J mice or SD rats. The reprogrammed LLCs at day 12 of culture were collected and resuspended in PBS for transplantation. About 1×10^6 cells/50μL PBS were transplanted into the parenchyma of recipient mice testis at 7 d post EDS-treatment. The EDS-treated mice that received TTFs were served as negative control. The serum were collected at 0, 7, and 14 d after transplantation.

To assess the intratesticular testosterone concentrations, we transplanted LLCs and TTFs into the testes of EDS-treated rats (1×10^6 cells/testis). After transplantation for 21 d, the serum and the interstitial fluid of animals were collected according to the previous method (50). The concentrations of testosterone were assayed by RIA method.

Transplantation of LLC to armpit of diabetic rats

To evaluate the potential benefits of LLCs on the improvement of diabetic-related phenotypes, STZ-induced type 2 diabetic rat model was used. The reprogrammed LLCs at day 12 were collected and encapsulated into the porous beads according to the instructions of Cell-in-a-Box Encapsulation Kit. Briefly, 2×10^6 cells were packed and resuspended in a 1.5 mL microcentrifuge tube with 1 mL Solution 1. The cell suspension was then dispensed in droplets into Solution 2 diluent. After dispensing the last droplet, stir for 5 min. The capsules were collected, washed five times by PBS and incubated in a 6-well plate with RIM 2 medium at 37°C for 24 h. These capsules were transplanted subcutaneously to armpit of the diabetic rats ($n = 5$, 2×10^6 cells/rat). The positive control group were the diabetic rats that had received a transplantation of TTFs. The concentrations of testosterone and fast blood glucose in serum were examined at 0, 7, 14, and 21 d after transplantation. The concentration of hemoglobin A1c (HbA1c) was also analyzed at 21 d using A1C Now$^+$ System (PTS Diagnostics, IN, USA).

Supplementary Material

Supplementary material is available at *PNAS Nexus* online.

Funding

Authors' Contributions

Z.S., H.C., and R.Z. conceived and designed the manuscript. Z.L., X.F., and X.G. performed all experiments. C.X. conducted all bioinformatics analyses. Z.L., R.Z., H.C., and Z.S. analyzed data, interpreted results of experiments, prepared figures. J.L., Y.H., and S.L. contributed tools, reagents, and materials. Z.S and H.C. wrote and revised the manuscript. All authors read and approved the final manuscript.

References

1. Dohle G, Arver S, Bettocchi C, Jones TH, Kliesch S. 2019. EAU guidelines on male hypogonadism. In European Association of Urology (EAU) guidelines [accessed by 9/18/2022]. http://uroweb.org/eau-guidelines/discontinued-topics/male-hypogonadism
2. Basaria S. 2014. Male hypogonadism. Lance. 383:1250–1263.
3. Petering RC, Brooks NA. 2017. Testosterone therapy: review of clinical applications. Am Fam Physician. 96: 441–449.
4. Chen PP, Zirkin BR, Chen HL. 2020. Stem Leydig cells in the adult testis: characterization, regulation and potential applications. Endocr Rev. 41:22–32.
5. Wang YY, Chen FF, Ye LP, Zirkin BR, Chen HL. 2017. Steroidogenesis in Leydig cells: effects of aging and environmental factors. Reproduction. 154:R111–R122.
6. Ye LP, Li XH, Li LX, Chen HL, Ge RS. 2017. Insights into the development of the adult Leydig cell lineage from stem Leydig cells. Front Physiol. 8:430.
7. Chen HL, Ge RS, Zirkin BR. 2009. Leydig cells: from stem cells to aging. Mol Cell Endocrinol. 306:9–16.
8. Chen H *et al.* 2019. Identification and functional characterization of microRNAs in rat Leydig cells during development from the progenitor to the adult stage. Mol Cell Endocrinol. 493: 110453.
9. U.S. Food and Drug Administration. 2019. FDA approves new oral testosterone capsule for treatment of men with certain forms of hypogonadism. [accessed 9/17/2022]. https://www.fda.gov/news-events/press-announcements/fda-approves-new-oral-testosterone-capsule-treatment-men-certain-forms-hypogonadism
10. Bhasin S *et al.* 2018. Testosterone therapy in men with hypogonadism: an endocrine society clinical practice guideline. J Clin Endocrinol Metab. 103:1715–1744.
11. Crawford PA, Sadovsky Y, Milbrandt J. 1997. Nuclear receptor steroidogenic factor 1 directs embryonic stem cells toward the steroidogenic lineage. Mol Cell Biol. 17:3997–4006.
12. Li L *et al.* 2019. Directing differentiation of human induced pluripotent stem cells toward androgen-producing Leydig cells rather than adrenal cells. Proc Natl Acad Sci USA. 116:23274–23283.
13. Ishida T *et al.* 2021. Differentiation of human induced pluripotent stem cells into testosterone-producing Leydig-like cells. Endocrinology. 162:bqab202.
14. Ge R *et al.* 2006. In search of rat stem Leydig cells: identification, isolation, and lineage-specific development. Proc Natl Acad Sci USA. 103:2719–2724.
15. Xia K *et al.* 2020. Restorative functions of autologous stem Leydig cell transplantation in a testosterone-deficient non-human primate model. Theranostics. 10:8705–8720.
16. Chen Y *et al.* 2019. Differentiation of human adipose-derived stem cells into Leydig-like cells with molecular compounds. J Cell Mol Med. 23:5956–5969.

17. Yang Y *et al*. 2017. Direct reprogramming of mouse fibroblasts toward Leydig-like cells by defined factors. Stem Cell Rep. 8:39–53.

18. Yang Y *et al*. 2020. Conversion of fibroblast into functional Leydig-like cell using defined small molecules. Stem Cell Rep. 15:408–423.

19. de Mattos K, Viger RS, Tremblay JJ. 2022. Transcription factors in the regulation of Leydig cell gene expression and function. Front Endocrinol (Lausanne). 13:881309.

20. Ge RS, Hardy MP. 1998. Variation in the end products of androgen biosynthesis and metabolism during postnatal differentiation of rat Leydig cells. Endocrinology. 139:3787–3795.

21. Ivell R, Wade JD, Ivell RA. 2013. INSL3 as a biomarker of Leydig cell functionality. Biol Reprod. 88:147.

22. Li ZH, Lu JD, Li SJ, Chen HL, Su ZJ. 2022. Generation of Leydig-like cells: approaches, characterization, and challenges. Asian J Androl. 24:335–344.

23. Jiang M *et al*. 2014. Characterization of Nestin-positive stem Leydig cells as a potential source for the treatment of testicular Leydig cell dysfunction. Cell Res. 24:1466–1485.

24. Eliveld J *et al*. 2019. Primary human testicular PDGFRα+ cells are multipotent and can be differentiated into cells with Leydig cell characteristics *in vitro*. Hum Reprod. 9:1621–1631.

25. Yang Y *et al*. 2015. Directed Mouse Embryonic stem cells into Leydig-like cells rescue testosterone-deficient male rats *in vivo*. Stem Cells Dev. 24:459–470.

26. Chen H, Wang Y, Ge R, Zirkin BR. 2017. Leydig cell stem cells: identification, proliferation and differentiation. Mol Cell Endocrinol. 445:65–73.

27. Li X *et al*. 2016. Regulation of seminiferous tubule-associated stem Leydig cells in adult rat testes. Proc Natl Acad Sci USA. 113:2666–7261.

28. Liu H *et al*. 2014. Basic fibroblast growth factor promotes stem Leydig cell development and inhibits LH-stimulated androgen production by regulating microRNA expression. J Steroid Biochem Mol Biol. 144:483–491.

29. Meinsohn MC, Smith OE, Bertolin K, Murphy BD. 2019. The orphan nuclear receptors steroidogenic factor-1 and liver receptor homolog-1: structure, regulation, and essential roles in mammalian reproduction. Physiol Rev. 99:1249–1279.

30. Weltner J *et al*. 2018. Human pluripotent reprogramming with CRISPR activators. Nat Commun. 9:2643.

31. Black JB *et al*. 2016. Targeted epigenetic remodeling of endogenous loci by CRISPR/Cas9-based transcriptional activators directly converts fibroblasts to neuronal cells. Cell Stem Cell. 19:406–414.

32. Yazawa T *et al*. 2019. Transcriptional regulation of ovarian steroidogenic genes: recent findings obtained from stem cell-derived steroidogenic cells. Biomed Res Int. 8973076.

33. Park BW *et al*. 2014. Ovarian-cell-like cells from skin stem cells restored estradiol production and estrus cycling in ovariectomized mice. Stem Cells Dev. 23:1647–1658.

34. Woods DC *et al*. 2013. Embryonic stem cell-derived granulosa cells participate in ovarian follicle formation *in vitro* and *in vivo*. Reprod Sci. 20:524–535.

35. Guo J *et al*. 2013. Comparison of cell types in the rat Leydig cell lineage after ethane dimethanesulfonate treatment. Reproduction. 145:371–380.

36. Mori H, Christensen AK. 1980. Morphometric analysis of Leydig cells in the normal rat testis. J Cell Biol. 84:340–354.

37. Navarro G, Allard C, Xu W, Mauvais-Jarvis F. 2015. The role of androgens in metabolism, obesity, and diabetes in males and females. Obesity (Silver Spring). 23:713–719.

38. Yeo S *et al*. 2021. Burden of male hypogonadism and major comorbidities, and the clinical, economic, and humanistic benefits of testosterone therapy: a narrative review. Clinicoecon Outcomes Res. 13:31–38.

39. Handgraaf S, Philippe J. 2019. The role of sexual hormones on the enteroinsular axis. Endocr Rev. 40:1152–1162.

40. Chang C, Yeh S, Lee SO, Chang TM. 2013. Androgen receptor (AR) pathophysiological roles in androgen-related diseases in skin, bone/muscle, metabolic syndrome and neuron/immune systems: lessons learned from mice lacking AR in specific cells. Nucl Recept Signal. 11:e001.

41. Navarro G *et al*. 2016. Extranuclear actions of the androgen receptor enhance glucose-stimulated insulin secretion in the male. Cell Metab. 23:837–851.

42. Xu W *et al*. 2020. Intracrine Testosterone activation in human pancreatic beta-cells stimulates insulin secretion. Diabetes. 69:2392–2399.

43. Krueger F, Andrews SR. 2011. Bismark: a flexible aligner and methylation caller for Bisulfite-Seq applications. Bioinformatics. 27:1571–1572.

44. Langmead B, Salzberg SL. 2013. Langmead. Bowtie2. Nat Methods. 9:357–359.

45. Hebestreit K, Dugas M, Klein HU. 2013. Detection of significantly differentially methylated regions in targeted bisulfite sequencing data. Bioinformatics. 29:1647–1653.

46. Park Y, Wu H. 2016. Differential methylation analysis for BS-Seq data under general experimental design. Bioinformatics. 32:1446–1453.

47. Zhou Y *et al*. 2019. Metascape provides a biologist-oriented resource for the analysis of systems-level datasets. Nat Commun. 10:1523.

48. Sakuma T, Nishikawa A, Kume S, Chayama K, Yamamoto T. 2014. Multiplex genome engineering in human cells using all-in-one CRISPR/Cas9 vector system. Sci Rep. 4:5400.

49. Tang XY *et al*. 2021. An UHPLC-MS/MS method for simultaneous determination of ten sex steroid hormones in ovariectomy-induced osteoporosis rat and its application in discovery of sex steroid hormones regulatory components of Xian-Ling-Gu-Bao capsule. J Pharm Biomed Anal. 195:113888.

50. Chung JY *et al*. 2020. Effects of pharmacologically induced Leydig cell testosterone production on intratesticular testosterone and spermatogenesis. Biol Reprod. 102:489–498.